Journal of Crystal Growth 343 (2012) 101–104

Contents lists available at SciVerse ScienceDirect

Journal of Crystal Growth

journal homepage: www.elsevier.com/locate/jcrysgro

Growth of vertical and defect free InP nanowires on $SrTiO_3$(001) substrate and comparison with growth on silicon

K. Naji [a,*], H. Dumont [a], G. Saint-Girons [a], J. Penuelas [a], G. Patriarche [b], M Hocevar [c], V. Zwiller [c], M. Gendry [a]

[a] Université de Lyon, Ecole Centrale de Lyon, Institut des Nanotechnologies de Lyon-INL, UMR5270/CNRS, 36 avenue Guy de Collongue, 69134 Ecully, France
[b] LPN-UPR20/CNRS, Route de Nozay, 91460 Marcoussis, France
[c] Quantum Transport, Kavli Institute of Nanoscience, Delft University of Technology, 2628CJ Delft, Netherlands

ARTICLE INFO

Article history:
Received 26 August 2010
Received in revised form
2 September 2011
Accepted 20 December 2011
Communicated by R.M. Biefeld
Available online 27 December 2011

Keywords:
A1. Crystal structure
A1. Nanostructures
A3. Molecular beam epitaxy
B1. Nanomaterials
B1. Perovskites
B2. Semiconducting III–V materials

ABSTRACT

We present a study of the molecular beam epitaxy of InP nanowires (NWs) on (001) oriented $SrTiO_3$ (STO) substrates using vapor liquid solid mechanism and gold–indium as metal catalyst. The growth direction of InP NWs grown on STO(001) is compared with NWs grown on (001) and (111) oriented silicon substrates. Gold–indium dewetting under a flux of indium results in the majority of InP NWs growing vertically from the surface of STO(001). With the growth parameters we have used the NWs have a pure wurtzite structure and are free of stacking faults and cubic segments. The structural quality of the NWs is confirmed by micro-photoluminescence measurements showing a narrow peak linewidth of 6.5 meV.

In recent years, the growth of III–V nanowires (NWs) on silicon (Si) [1] by Vapor Liquid Solid (VLS) mechanism [2,3] has excited much interest because it could allow integrating optoelectronic and photonic functionalities with Si technologies, circumventing the fundamental issues related to lattice mismatch, antiphase boundaries and thermal expansion [4,5]. To facilitate the encapsulation and contacting of NWs in future devices or to obtain homogeneous radial growth by molecular beam epitaxy (MBE), great efforts have been made to control the NWs growth direction and to favor the vertical growth direction [6–9]. Many groups have obtained vertically oriented III–V NWs on Si(111) [10,11] because the NWs grow preferentially in the $\langle 111 \rangle$ directions and because the [111] growth direction lying perpendicular to the (111) surface of the substrate can be selected among the other $\langle 111 \rangle$ orientations by adjusting the growth conditions [6,7]. On the contrary, it seems to be difficult to obtain vertically oriented NWs on Si(001) by VLS assisted growth with gold as metal catalyst. The observed inclined growth directions of NWs have been explained by an eutectic reaction between gold and silicon during the dewetting [1]. This reaction reveals {111} facets at the Si substrate surface under the catalyst droplets and it is argued [1] that the NWs growth is initiated on these {111} facets and that the NWs grown on Si(001) are inclined following the four equivalent $\langle 111 \rangle$ directions of the cubic structure of silicon. Obtaining vertically standing NWs on Si(001) thus remains an important objective to integrate them on silicon.

In this work, we propose an original solution to achieve this objective. Our strategy consists in using a thin (001)-oriented $SrTiO_3$ (STO) buffer layer grown on Si(001) [12,13], typically 1–2 nm-thick, acting as a template to control the NWs growth orientation and to enhance the growth of vertically standing InP NWs on Si(001). The choice of a crystalline STO(001) layer is motivated by recent results [14] concerning the structural properties of InP grown on STO(001) surfaces: InP is (111)-oriented on unreconstructed STO(001) surfaces, and is (001)-oriented on (2×1)-reconstructed (001) STO surfaces. Unreconstructed STO(001) surface could thus lead to the vertical growth of (111)-oriented InP NWs on Si(001). Another advantage in using a STO template is related to the specificity of mismatch accommodation at the InP/STO interface [15]: when grown on STO, InP takes its bulk lattice parameter as soon as growth begins without any formation of threading defects related to plastic relaxation. Using an STO template to integrate InP NWs on Si(001) could thus bypass the effect of high lattice mismatch between InP and Si and

* Corresponding author. Tel.: +33 620208573.
E-mail address: khalid_n18@hotmail.com (K. Naji).

0022-0248/$ - see front matter © 2011 Elsevier B.V. All rights reserved.
doi:10.1016/j.jcrysgro.2011.12.062

the related effect of critical diameter reported for NWs grown on Si [16]. In this context, we report here a study of the VLS assisted MBE growth of InP NWs on STO(001) substrates using gold–indium (Au–In) as catalyst. The structural and optical properties of these NWs are compared to those of InP NWs grown on (001) and (111) oriented Si substrates. The influence of Au–In dewetting on the composition of the catalyst droplets at the initial stage of the NWs growth on STO and consequently on the orientation of the InP NWs is also discussed.

The NWs samples were grown in a solid source MBE reactor equipped with a valved cracked cell for phosphorus and reflexion high energy electron diffraction (RHEED) facilities. Before metal catalyst deposition, the STO substrates were etched into a buffered oxide etching (BOE) solution in order to obtain a TiO_2 terminated STO(001) surface. Si(001) and Si(111) substrates were etched with a fluoridric acid solution to remove the natural oxide from their surface. After chemical treatment, the substrates were loaded into a metal sputtering chamber. A 2 nm-thick Au/In double layer was deposited on STO(001), Si(001) and Si(111) substrates. The Au–In dewetting was then realized in the MBE chamber to form the catalyst droplets. For this purpose, Si(001) and Si(111) substrates were annealed in the MBE chamber at 600 °C for 15 mn and the STO(001) substrates were annealed at 750 °C during 15 mn. The InP NWs were then grown during 10 mn at 380 °C with an indium beam equivalent pressure (BEP) of 7.5×10^{-7} torr and a phosphorus BEP of 1.2×10^{-5} torr, corresponding to a high V/III BEP ratio equal to 16. Scanning electron microscopy (SEM), high resolution transmission electron microscopy (HRTEM) and X-ray diffraction (XRD) were used to characterize the structural properties of the NWs. HRTEM measurements were performed on a 200 kV Philips CM20 microscope. XRD measurements were performed using a Rigaku Smartlab machine having an in-plane scattering arm. The X-ray source is a rotating anode operating at 9 kW, monochromatized with a two reflection Ge(220) crystal, which select the Cu Kα1 radiation (wavelength = 1.5406 Å). Optical properties of single InP NWs transferred on SiO_2 template were investigated by microphotoluminescence (μPL) measurements at 10 K using a green laser (532 nm).

Figs. 1a and b show the top view SEM images of InP NWs grown on Si(001) and Si(111) substrates, respectively. We can note that a rough InP layer is grown between the NWs as often observed during the VLS growth of NWs by MBE. Concerning the growth direction of the NWs, the four equivalent ⟨111⟩ growth directions are detected on Si(001) (Fig. 1a). These orientations correspond to the four ⟨111⟩ directions typically observed for NWs grown on a (001)-oriented surface. On Si(111), the SEM image (Fig. 1b) exhibits bright spots corresponding to the top of vertical NWs. As expected on Si(111), a majority of NWs grow perpendicularly to the substrate surface.

On STO(001) substrates, two samples (STO1 and STO2) were grown using two different dewetting procedures of the Au/In double layer at 750 °C in the MBE chamber. For STO1 sample the dewetting was carried out under ultra high vacuum, while for STO2 sample the dewetting was carried out under an indium flux corresponding to a BEP of 1.3×10^{-7} torr. The RHEED pattern of STO1 sample before growth at 380 °C was spotty, indicating that the catalyst particles presented a solid crystalline structure. We assume that the indium of the double layer is desorbed during dewetting at 750 °C and that the catalyst particles are pure solid gold. On the contrary, for STO2 sample with dewetting under an indium flux, the RHEED pattern before the growth at 380 °C was

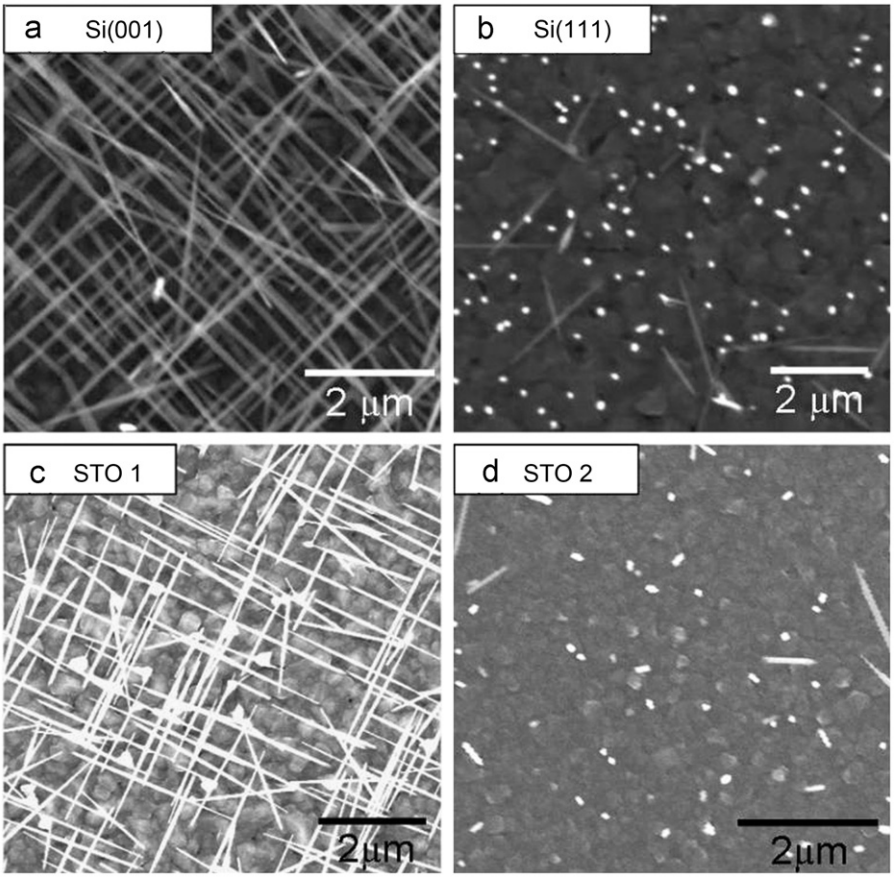

Fig. 1. Top view SEM images of InP NWs grown on: (a) Si(001), (b) Si(111), (c) STO1 sample and (d) STO2 sample.

diffuse, indicating that the catalyst was liquid. Even if an eutectic point is near 425 °C in the Au–In phase diagram, it was already observed that Au–In alloys can be liquid at temperature as low as 380 °C [17]. Consequently, we assume that dewetting under the indium flux enables keeping the Au–In droplet composition leading to the liquid phase indicated by the RHEED pattern.

The InP NWs were then grown on STO1 and STO2 samples in the same conditions as those used on Si substrates. Top-view SEM images of the STO1 and STO2 samples after the growth, are displayed in Figs. 1c and d, respectively. As on Si substrates, we can observe that a rough InP layer is grown between the NWs. For STO1 sample, SEM image shows that the InP NWs have the four growth directions similar to those observed on Si(001). On the contrary, SEM image of STO2 sample shows about 80% of vertical InP NWs (in Fig. 1d). We can conclude that the indium composition of the catalyst particles before growth has a strong effect on the growth direction of the InP NWs grown on STO.

HRTEM images were obtained from InP NWs grown on STO(001) and Si(001) substrates with diameter in the 20–40 nm range. Fig. 2 shows the results obtained on InP NWs grown on STO(001). As evidenced by the selected area electron diffraction (SAED) patterns (Fig. 2a), the NWs have a wurzite (WZ) structure with the [0001] axis along the growth direction (Fig. 2b) whatever the substrate.

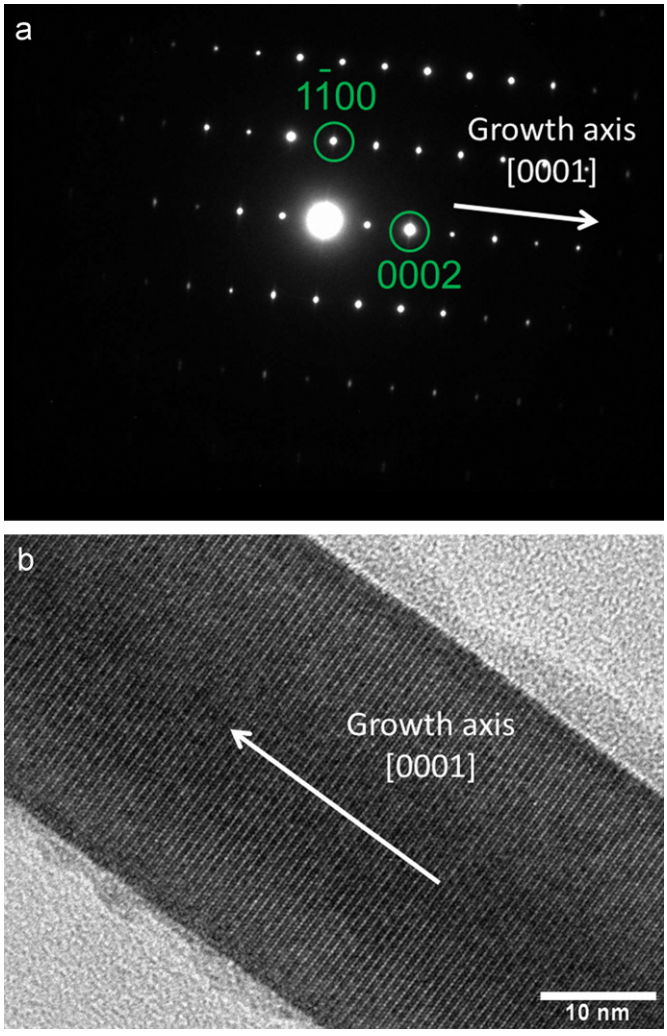

Fig. 2. (a) SAED pattern with indexation of the main diffraction spots and (b) HRTEM image of InP NWs grown on STO(001).

To confirm the vertical growth direction of the InP NWs grown on STO with dewetting under indium flux, out of plane and grazing incidence X-ray diffraction was performed on a third sample (STO3) similar to STO2 sample, with about 60% of vertical NWs and 40% of inclined NWs. Fig. 3a shows the out of plane

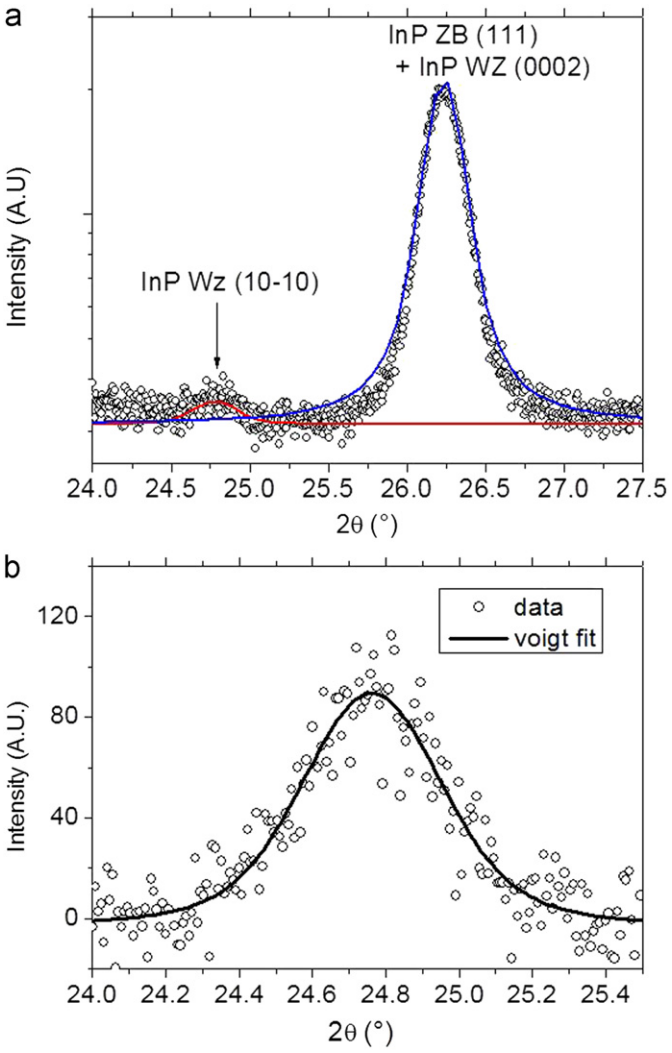

Fig. 3. X-ray diffraction pattern of STO3 sample: (a) out of plane geometry, (b) grazing incidence geometry. Data were fitted with Voigt function and linear background.

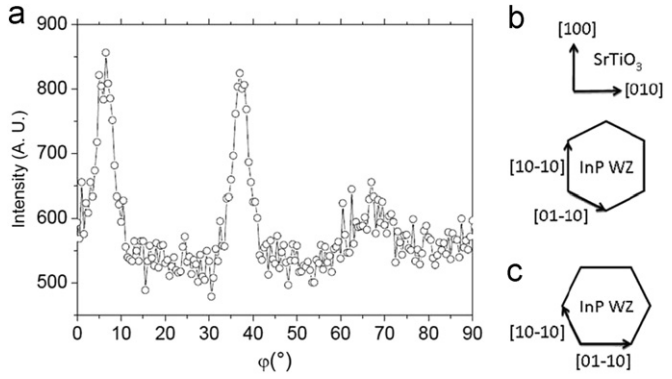

Fig. 4. (a) Azimuthal scan performed on STO3 sample at grazing incidence and at a Bragg angle corresponding to (10−10) InP reflections. (b) and (c): Schematic representation of the two different kinds of epitaxial relationship with STO for the vertical NWs.

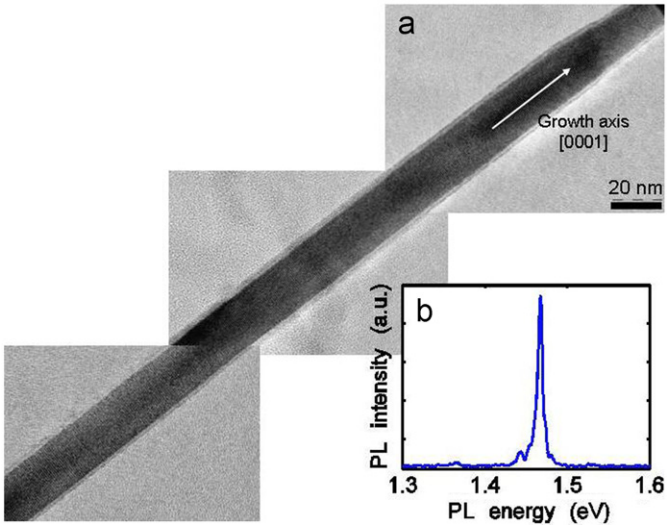

Fig. 5. (a) HRTEM image and (b) μPL spectrum at 10 K of a single InP NW grown on STO(001). The excitation power is 13.6 W/cm^2.

diffraction pattern of STO3 sample. Two peaks are identified and related to the (10−10) WZ reflection at $2\theta=24.78^\circ$ and (0002) WZ+(111) ZB reflections at $2\theta=26.23^\circ$, respectively. The (10−10) WZ reflection at $2\theta=24.78^\circ$ corresponds to NWs oriented parallel to the surface, which could be attributed to broken NWs during sample manipulation (a WZ inclusion in the rough InP layer having this orientation seems not probable). The second peak ($2\theta=26.23^\circ$) is mostly due to the (111) ZB reflection coming from the rough InP layer. In fact, the diffracted signal from NWs is very weak compared with that of the rough InP layer. From the fitting of this peak, the lattice parameter of the rough InP layer is equal to 0.5879 nm, which is very close to the bulk value in accordance with the specificities of the III–V semiconductor/STO hetero-interface [15]. In order to increase the signal from InP NWs and to obtain a direct measurement of the in-plane lattice parameter of vertical NWs, surface X-ray diffraction was performed at a grazing incidence of 0.3° (slightly below the critical angle for total reflection). The Fig. 3b shows the (10−10) Bragg peak of the vertical NWs. By fitting the data with a Voigt function, the center and the width of the peak were extracted. The peak center is located at $2\theta=24.76^\circ$, which corresponds to an in-plane lattice parameter equal to 0.4148 nm, in accordance with the bulk value (0.4150 nm [18]).

To gain information about the epitaxial relationship between these NWs and the STO substrate, an azimuthal scan along the φ axis was performed, i.e. the sample was turned in his surface plane and the Bragg angle kept constant at $2\theta=24.76^\circ$, with the same incidence angle of 0.3° (Fig. 4a). Interestingly a 12-fold symmetry is observed, which can be explained by the presence of two different kinds of epitaxial relationship with STO for the vertical NWs (Figs. 4b and c). The first epitaxial relationship corresponds to InP WZ [10−10]//STO [100] (Fig. 4b) and the second one to InP WZ [01−10]//STO [010] (Fig. 4c). Interestingly, this interface structure was already observed in our previous studies [15,19] for a cubic InP lattice (InP ZB [110]//SrTiO3 [100]), which results in the formation of 111-oriented or 001-oriented cubic InP lattice. We showed that it was possible to favor the 111-orientation using high phosphorous BEP. For the NW growth we used a phosphorus BEP equal to 1.2×10^{-5} torr, which is quite high to lead to the 111-orientation inducing the growth of vertical NWs.

Concerning the structural quality of the NWs, the same tendency can be observed on Si and STO substrates. For the growth temperature and the high V/III BEP ratio we have used, the NWs are defect-free of stacking-faults and cubic segments. The defect-free structure for InP NWs grown on STO was verified along the whole 1–2 μm length of the NWs (Fig. 5a). A typical μPL spectrum at 10 K of a single InP NW from STO2 sample with excitation intensity equal to 13.6 W/cm^{-2} is shown in Fig. 5b. The spectrum shows only one peak at 1.465 eV, which corresponds to the WZ structure of the NW. We observe a narrow emission linewidth of 6.5 meV indicating good structural quality of the InP NWs without any zinc-blend segments. These measurements confirm the high structural quality of the InP NWs grown on STO(001) as evidenced by the TEM observations.

In summary, vertical and defect-free InP NWs have been grown on STO(001) substrates with gold–indium catalyst. The effect of the indium composition of the catalyst droplets on the growth direction of InP NWs on STO has been evidenced. However, our results demonstrate that growing vertical InP NWs on a crystalline STO(001) surface is possible. With chosen growth conditions, defect-free wurtzite NWs were grown on STO similarly to NWs grown on Si substrate. The μPL measurements show intense single wire luminescence and confirm that the NWs grown on STO have good structural properties. These results show that using a crystalline STO template grown on Si(001) could be well adapted for the integration of vertical InP NWs on Si(001).

References

[1] A.L. Roest, M.A. Verheijen, O. Wunnicke, S. Serafin, H. Wondergem, E.P.A.M. Bakkers, Nanotechnology 17 (2006) S271.
[2] R.S. Wagner, W.C. Ellis, Applied Physics Letters 4 (1964) 5.
[3] V.G. Dubrovskii, N.V. Sibirev, J.C. Harmand, F. Glas, Physical Review B 78 (2008) 235301.
[4] S.F. Fang, K. Adomi, S. Lyer, Z. Morkoc, H. Choi, C. Otsuka, Journal of Applied Physics 68 (1990) R31.
[5] D. Cohen, C.B. Carter, Journal of Microscopy 208 (2002) 84.
[6] K. Tomioka, J. Motohisa, S. Hara, T. Fukui, Nano Letters 8 (2008) 3475.
[7] S.T. Boles, C.V. Thompson, E.A. Fitzgerald, Journal of Crystal Growth 311 (2009) 1446.
[8] J. Bai, J.S. Park, Z. Cheng, M. Curtin, B. Adekore, M. Carroll, A. Lochtefeld, M. Dudley, Applied Physics Letters 90 (2007) 101902.
[9] U. Krishnamachari, M. Borgstrom, B.J. Ohlsson, N. Panev, L. Samuelson, W. Seifert, M.W. Larsson, L.R. Wallenberg, Applied Physics Letters 85 (2004) 2077.
[10] G. Deppe, N. Holonyak Jr., D.W. Nam, K.C. Hsieh, G.S. Jackson, R.J. Matyi, H. Shichijo, J.E. Epler, H.F. Chung, Applied Physics Letters 51 (1987) 637.
[11] S.M. Ting, E.A. Fitzgerald, Journal of Applied Physics 87 (2000) 2618.
[12] G. Niu, G. Saint-Girons, B. Vilquin, G. Delhaye, J.-L. Maurice, C. Botella, Y. Robach, G. Hollinger, Applied Physics Letters 95 (2009) 062902.
[13] G. Delhaye, C. Merckling, M. El-Kazzi, G. Saint-Girons, M. Gendry, Y. Robach, G. Hollinger, L. Largeau, G. Patriarche, Journal of Applied Physics 100 (2006) 124109.
[14] J. Cheng, P. Regreny, L. Largeau, G. Patriarche, O. Mauguin, K. Naji, G. Hollinger, G. Saint-Girons, Journal of Crystal Growth 311 (2009) 1042.
[15] .G. Saint-Girons, J. Cheng, P. Regreny, L. Largeau, G. Patriarche, G. Hollinger, Physical Review B 80 (2009) 155308.
[16] L.C. Chuang, M. Moewe, C. Chase, Applied Physics Letters 90 (2007) 043115.
[17] M. Tchernycheva, L. Travers, G. Patriarche, F. Glas, J.C. Harmand, G.E. Cirlin, V.G. Dubrovskii, Journal of Applied Physics 102 (2007) 094313.
[18] M.W. Larson, J.B. Wagner, M. Wallin, P. Hakansson, L.E. Froberg, L. Samuelson, L.R. Wallenberg, Nanotechnology 18 (2007) 015504.
[19] A. Chettaoui, J. Penuelas, B. Gobaut, J. Cheng, A. Benamrouche, Y. Robach, G. Hollinger, G. Saint-Girons, Surface Science 605 (2011) 912.